# Natural product-based pressure-sensitive adhesives via carveol-dithiothreitol thiol-ene step-growth polymerization

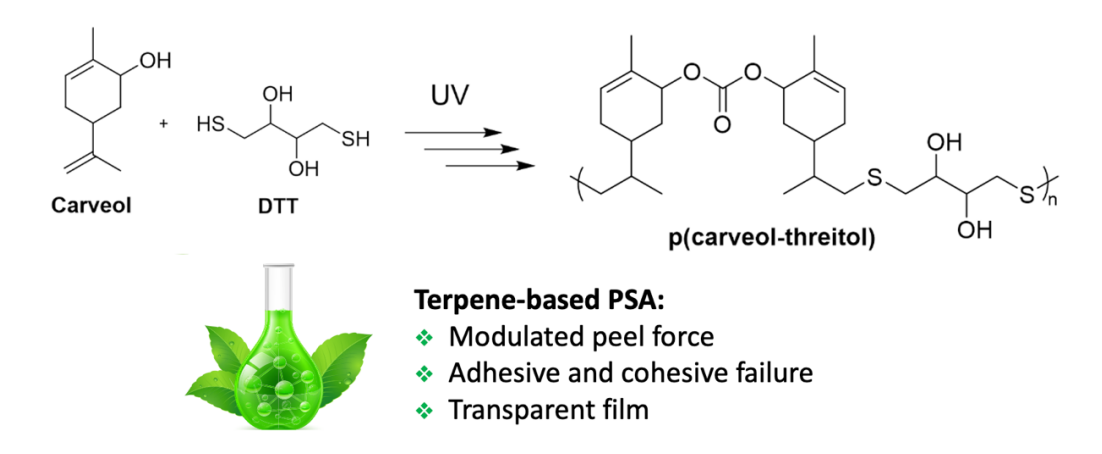
Emily A. Prebihalo, Theresa M. Reineke\*

Department of Chemistry, University of Minnesota, 207 Pleasant St. SE, Minneapolis, MN 55455,

#### USA.

Corresponding author: treineke@umn.edu

## TOC:



#### Abstract:

Pressure-sensitive adhesives occupy a large role in commercial use of polymers, however they are typically limited to non-degradable formulations using petroleum-based materials. As the plastic and environmental crises have intensified, the need for renewable starting materials and degradable designs have similarly deepened. With that goal, we endeavored to make adhesive films out of renewable terpenes as a safer and more sustainable route to PSAs. Specifically, based on our previous report of the crosslinking ability of a carveol-based carbonate through thiol-ene chemistry, we report further exploration of the adhesive possibilities of this system. A carbonate monomer of dimerized carveol was linearly polymerized with dithiothreitol *via* UV-initiated thiol-ene chemistry and formed into adhesive coatings, with unmodified geraniol doped in as a tackifier. We obtained a range of adhesive properties based on the ratio of *exo*-methylene to thiol units and report on the degradation of the adhesive coatings.

The polymer industry has been heavily reliant on fossil fuel-derived materials since its inception. With the rising attention on the climate crisis, strategies towards reducing petroleum dependence have become central to the materials science community. Concurrently, the lack of

ready degradation in the vast majority of polymeric products has come to a tipping point with societal awareness of the plastic crisis,<sup>2</sup> calling for plastic products to incorporate a meaningful end-of-life pathway within their design.<sup>3,4</sup> These approaches have permeated all applications of polymers, including pressure sensitive adhesives (PSAs).<sup>5</sup> PSAs are soft polymeric products that flow upon application and adhere to a substrate with pressure applied over a short time period.<sup>6</sup> They tend to be lightly crosslinked acrylics<sup>7</sup> or triblock architectures<sup>8,9</sup> and must balance viscosity and elasticity to provide easy application but adhesive strength. Adhesives occupy a wide range of applications, largely dependent on the force measured upon removal and the mode of failure: either adhesive or cohesive. Adhesive failure occurs between the substrate and PSA, while cohesive failure occurs within the PSA, leaving residue on the substrate after removal.<sup>10</sup> Most commercial PSAs consist of a base polymer with tackifiers, plasticizers, and any other needed additives to fine-tune the thermal and adhesive properties.<sup>11</sup>

Adhesives have historically been made using petroleum-derived materials without endof-life considerations. Recent work has begun to delve into renewable alternatives, 12-14 such as vegetable oils, 15-18 lignin, 6 and lactides. 19-21 Previous work from our group has highlighted the use of sugars in PSAs through a triblock architecture. Gallagher et al. showed the use of acrylated isosorbide as the high  $T_g$  block with *n*-butyl acrylate as the rubbery midblock to yield adhesive films with peel forces of up to 2.9 N/cm, similar to commercial triblock standards. <sup>10</sup> Similarly, Nasiri et al. utilized an acrylated glucose as the end blocks surrounding a low  $T_g$  n-butyl actylate block, reaching up to 2.3 N/cm peel forces.<sup>22</sup> Extending the use of renewable resources to all three blocks, Sajjad et al. demonstrated the synthesis of a triblock PSA composed of a triacetic acid lactone hard block with lauryl acrylate utilized as the soft midblock.<sup>23</sup> With the addition of a rosin ester tackifier, these films reached up to 7.6 N/cm under peel adhesion tests. Inspired by this previous work, as well as our recent report of the crosslinking of terpene-based monomers using thiol-ene chemistry,<sup>24</sup> we sought to leverage the tackiness of terpenoid resins observed previously to pursue PSA applications. Terpenoids are isolated from plants and lauded for their variety of architectures and low toxicity, and have been used in adhesives previously, most commonly as a tackifier when used as a polyterpene resin.<sup>25–27</sup> Terpenes have also been incorporated into the main chain of PSAs primarily in acrylated versions copolymerized into a triblock architecture, although this is largely limited to tetrahydrogeranyl acrylate as the low  $T_{\rm g}$ component.<sup>28–31</sup> There are fewer reports on the incorporation of varied terpenes into the backbone of the main PSA component<sup>32,33</sup> and a need to increase the systematic study of terpene-based polymers as inherent PSAs to expand the scope of terpenes studied for adhesive applications.

To address this need for further investigation of terpenes as adhesive materials, we targeted the use of modified terpenes in radical thiol-ene step-growth polymerization to form pressure-sensitive adhesives. Specifically, we utilized carveol, a monocyclic terpenoid found in essential oils such as caraway.<sup>34</sup> Carveol is cheap, non-toxic, has been shown to have antioxidant and cytoprotective effects,<sup>35</sup> and has an *exo*-methylene unit to facilitate a thiol-ene reaction. We hypothesize that the cycloaliphatic nature could confer some mechanical strength to adhesive formulations. Our choice of thiol, dithiothreitol (DTT), is attractive for its relatively low odor and the incorporation of free hydroxyls, shown to promote adhesion.<sup>17</sup> Thus, here we employ a carveol-based alkene monomer and dithiothreitol to achieve adhesives suitable for film

formation. Linear thiol-ene polymerizations were investigated through a step-growth mechanism after observation of only the *exo*-methylene unit showing reactivity under thiol-ene. To reduce solvent usage we use crude polymerization solutions directly for coating formulation, to avoid lengthy purification followed by re-dissolution of polymers into a formulation. To further increase the terpeoide usage, we utilized unmodified geraniol as an additive in the formulation to investigate the range of adhesive properties possible with this terpene-based PSA. Herein, we report the synthesis of carveol-based coatings through thiol-ene chemistry that show modulable adhesive properties, including peel forces comparable to a commercial sticky note. To the best of our knowledge this is the first report of a carveol-based monomer for use in PSAs, particularly without acrylate functionalization. This work represents an expansion of the use of terpenes in PSAs from acrylated triblocks and tackifiers to backbone units through thiol-ene polymerization.

Beginning from carveol, a functionalized alkene monomer was synthesized as reported previously<sup>36</sup> to yield di-carveol-carbonate (DCC), a dimerized version of carveol linked by a degradable carbonate unit. This synthesis is a simple two-step process using benign solvents and only one stage of purification, however it does involve the use of carbonyldiimidazole (CDI). While CDI has less desirable sustainability traits, the simplicity of synthesis along with limited purification required necessitated its use. The thiol-ene polymerization of DCC and DTT under UV conditions was investigated first (Figure 1a). Solutions were formed in a closed vial and exposed to UV light while stirring using a MelodySusie 36 W UV Nail Dryer at 365 nm. The DCC monomer contains four alkenes total, consisting of two exo-methylene units and two internal tri-substituted alkenes. Upon analysis via NMR, the exo-methylene protons were consumed during polymerization but no change to the tri-substituted alkenes was observed (Figure 1b). Based on this, it was concluded that linear polymers were being formed. <sup>37–39</sup> Via IR analysis the carbonate stretch remains unchanged after polymerization while the exo-methylene and free thiol stretches significantly decrease or disappear (Figure 1c). To investigate this stepgrowth system, polymerizations were performed using an excess of thiol reagent in a 1:2 exomethylene:-SH ratio (referred to as 1:2 exo:-SH) to target full conversion of the less reactive exomethylene units. Polymerizations were run in methyl ethyl ketone (MEK) at varying concentrations and using the photoinitiator (2,4,6-Trimethylbenzoyl)diphenylphosphine oxide (TPO) at various loadings (Table 1). Polymerizations were tracked by NMR to monitor conversion before being purified for full characterization. Additionally, as we endeavored to prioritize sustainability, only polymerizations with a suitable crude solution viscosity for coating formation were taken forward for purification and characterization. Within each concentration, the maximum conversion (100%) was reached with 0.05 equivalents of photoinitiator relative to DCC present, correlating with the highest  $M_n$  by MALS-SEC (Table 1). At the lower concentration of 1 M, molar masses were predictably lower at equivalent conversions. Taking these results forward, polymerizations were performed at a 1:1 exo:-SH ratio, using 0.05 equivalents TPO and 1.5 M in MEK as the optimized system. At the same UV irradiation time, the 1:1 system showed lower NMR conversion (78%), thus the UV exposure was increased to 30 minutes. At this longer exposure time conversion repeatedly and consistently reached 82%, hypothesized to be due to terminations and side reactions when there is not an excess of thiol present, as well as diffusion limitations. Predictably, the molar mass at 82% conversion was significantly larger than at 78%, thus all future polymerizations for the 1:1 system were

irradiated for 30 minutes. The thermal properties of these linear polymers all showed the temperature at 5% mass loss ( $T_{d,5\%}$ ) to be around 170 °C by thermogravimetric analysis (TGA) and glass transition temperatures ( $T_g$ ) around 30-40 °C *via* differential scanning calorimetry (DSC). These similar Tg values show a slight dependence on molar mass, with the low molar mass samples having Tg values at the lower end and any polymers with a molar mass of 10-20 kDa showing a Tg around 40 °C. However, Tg values represent a range of a thermal transition thus the tight grouping of values is difficult to pull any concrete trends from. Typically, PSA formulations require  $T_g$  values between -5 and -60 °C to give good tack,<sup>33</sup> therefore these  $T_g$  values are markedly higher than what is expected and warranted more thorough investigation of the synthesized coatings.

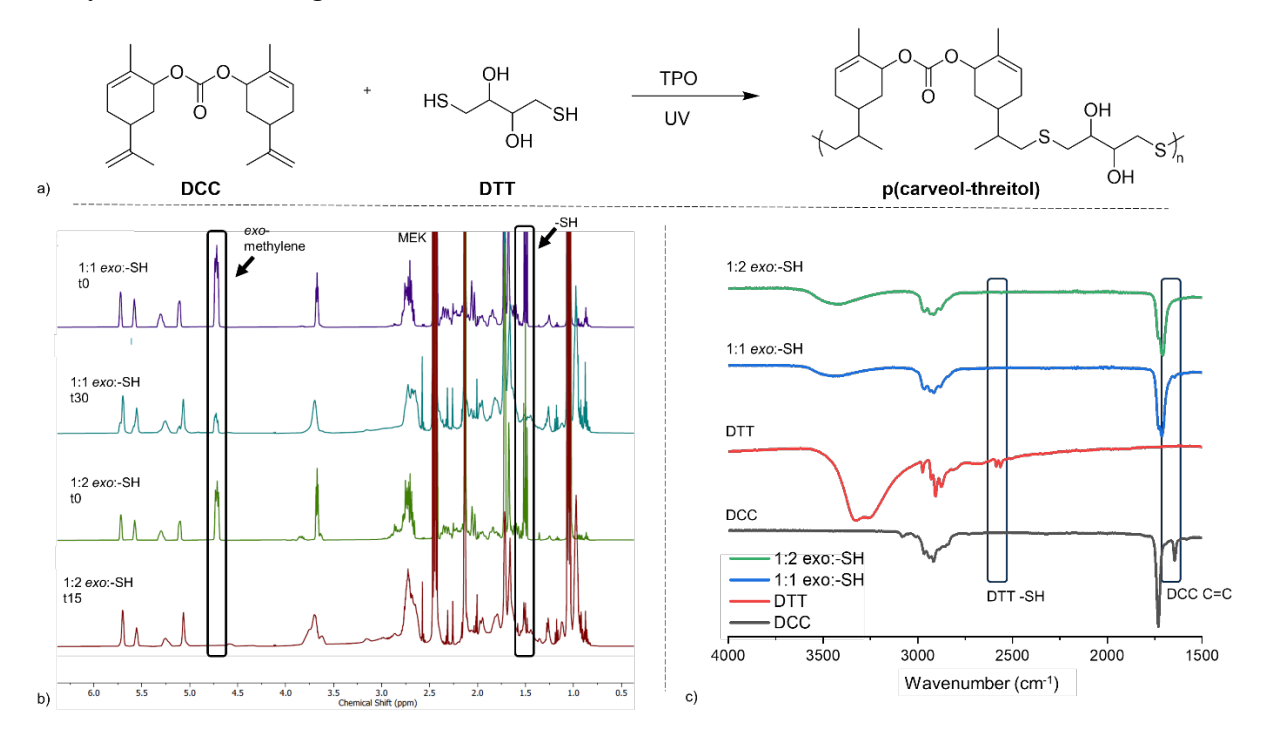


**Figure 1**. a) Polymerization scheme of DCC and DTT under UV conditions using TPO as a photoinitiator b) <sup>1</sup>H NMR spectra of polymerizations at 1:1 and 1:2 *exo*:-SH ratios at time=0 and at full reaction c) IR spectra of DCC and DTT monomers with polymerizations at 1:1 and 1:2 *exo*:-SH ratios

Exo:- SH	Initiator loading (eq)	MEK concentration (M)	UV exposure (min)	Conversion (NMR)	M <sub>n,SEC</sub> (kDa)	Ð	T <sub>d,5%</sub> (°C)	T <sub>g</sub> (°C)
1:2	0.09	1.5	15	98%	16.7	1.2	171	42
1:2	0.05	1.5	15	100%	19.8	1.2	166	42
1:2	0.01	1.5	15	98%	4.13	3.4	166	29

1:2	0.09	1	15	98%	10.1	2.3	165	40
1:2	0.05	1	15	100%	11.5	1.7	169	41
1:2	0.01	1	15	95%	4.40	1.7	170	35
1:1	0.05	1.5	15	78%	6.4	1.8	172	35
1:1	0.05	1.5	30	82%	20.5	1.8	169	40

**Table 1.** Polymerization conditions for linear thiol-ene. *Exo*:-SH refers to the ratio of *exo*-methylene alkenes to free thiols in DTT.

Adhesive coatings were formed by performing the polymerization as above in MEK using 0.05 equivalents of photoinitator and UV exposure times of 15 or 30 minutes for 1:2 and 1:1 ratios, respectively, to reach maximum monomer conversion, based on the conditions that reached the highest molar masses in Table 1. The crude solution was allowed to cool to room temperature and any tackifier was added in and mixed thoroughly. Crude solutions were taken directly forward to form coatings by using a tape coater onto a poly(ethylene terephthalate) (PET) backing sheet. Coatings were then left to dry for 2 days and tested for peel adhesion and further characterization.

Screening conditions for coating properties occurred within the 1:2 exo:-SH system with no tackifiers added, beginning with a coating thickness of 100 µm, and screening lower UV exposure times to investigate a range of conversions less than 100% and their effect on the adhesive properties. All coatings were transparent and colorless after drying (see Figure S18 for representative photos), and were tested for adhesion by application to a stainless steel plate with a weighted roller. When exo-methylene conversion was less than 100% the coating showed cohesive failure, with cohesive forces of 1.0 and 1.23 N/cm for 80% and 89% conversion, respectively. When conversion was increased to 100% the coating showed adhesive failure, whether the solution was made in 1 M or 1.5 M MEK, with a slight increase in adhesive force at the higher concentration. A similar trend held when geraniol was added in as a tackifier at 10 mol%. Both at 1 M and 1.5 M the coatings showed a mix of adhesive and cohesive failure, with the forces of each failure mode increasing at the higher concentration. Notably, in the mixed failure systems the adhesive failure occurred at the edges of the coating, where it is likely to have spread out to a thinner layer. Therefore, to target more adhesive failure, the coating thickness was decreased from 100 µm to 75 µm. Here, at 77% and 90% conversion the coating showed a mix of cohesive and adhesive failure, in contrast to the 100 µm films. As expected, the coatings at 90% conversion showed higher peel forces in both the adhesive and cohesive sections than the coatings at 77% conversion (Table 2). Based on the results of the purified polymer characterizations, we endeavored to push the system to full conversion to reach maximum molar mass, as established in Table 1. At 100% conversion the coatings showed fully adhesive failure, even at 100 µm thickness. By decreasing the coating to 75 µm the peel force increased from 0.17 N/cm to 0.39 N/cm while still showing completely adhesive failure. Notably, the error bars

significantly decrease at 100% conversion, showing more repeatable and consistent coatings are being formed. These results match that of a commercial sticky note tested in identical conditions as a control (0.35 N/cm, Figure 2). Further analysis of these coatings show that while all of the *exo*-methylene is consumed, nearly all of the free thiol in DTT is also consumed, even while present in a large excess to the reactive *exo*-methylene unit. These dried coatings did not fully dissolve in CDCl<sub>3</sub>, indicating some amount of crosslinking may be occurring over the course of the drying period. An IR spectrum shows a stretch at 515 cm<sup>-1</sup> (Figures S19-20), previously reported to correspond to a S-S stretch,<sup>40,41</sup> and suggesting disulfide formation of the remaining free thiol after all *exo*-methylenes have reacted.<sup>42</sup>

Notably, many PSAs require small amounts of crosslinking to confer adhesive strength and the extent of crosslinking modulates the balance between adhesive and cohesive behavior. 43–45 We note that as the monomer conversion increases in these systems, the failure mode becomes more adhesive and the peel force increases, indicating more crosslinking is occurring. However, if the crosslinking increases too much, the coating loses its adhesive properties, as we discovered in our early experiments. The coatings shown here have been optimized to have a crosslinking level appropriate for adhesive behavior.

Exo:- SH	Coating thickness (µm)	MEK conc. (M)	Conversion (NMR)	Tackifier	T <sub>d,5%</sub> (°C)	T <sub>g</sub> (°C)	Failure mode	Adhesive force (N/cm)	Cohesive force (N/cm)
1:2	100	1.5	80%	N/A	-	-	Coh.	-	1.00
1:2	75	1.5	77%	N/A	-	-	Mix	2.37	1.83
1:2	100	1.5	89%	N/A	-	-	Coh.	_*	1.23
1:2	75	1.5	90%	N/A	-	-	Mix	2.89	2.95
1:2	100	1	100%	N/A	-	-	Adh.	0.11	-
1:2	100	1.5	100%	N/A	-	-	Adh.	0.17	-
1:2	100	1	100%	10 mol% geraniol	-	-	Mix	1.35	0.98
1:2	100	1.5	100%	10 mol% geraniol	-	-	Mix	1.82	2.48
1:2	75	1.5	100%	N/A	140	-8	Adh.	0.39	-
1:2	75	1.5	100%	BHT	121	-10	Adh.	0.27	-
1:2	75	1.5	100%	10 mol% rosin ester	132	-14	Adh.	0.35	-
1:2	75	1.5	100%	10 mol% geraniol	120	-15	Adh.	0.27, 4.52	-
1:2	75	1.5	100%	20 mol% geraniol	149	-17	Mix	2.33	3.02
1:2	75	1.5	100%	30 mol% geraniol	157	-24	Mix	2.0	2.51
1:1	75	1.5	82%	N/A	128	0	Adh.	0.09	-
1:1	75	1.5	82%	10 mol% rosin ester	128	-6	Adh.	0.14	-
1:1	75	1.5	82%	10 mol% geraniol	151	-9	Adh.	0.15	-

1:1	75	1.5	82%	20 mol% geraniol	149	-17	Coh.	-	1.58
1:1	75	1.5	82%	30 mol% geraniol	144	-27	Coh.	-	0.09

**Table 2.** Coating formulations and results. \*one adhesive peak at the beginning of the curve, not being represented here. \*\*two modes of adhesive failure present

Armed with this optimization, coatings at 1:2 and 1:1 exo:-SH ratios were investigated with varying levels of tackifier added, beginning with 10, 20, and 30 mol% geraniol (Table 2). In the 1:2 exo:-SH system as geraniol was added the failure mode became more cohesive, and a maximum peel force was reached at 20 mol%. Notably, as occurred with the no tackifier systems when the 10 mol% geraniol coating was cast at 100 µm the film showed a mix of cohesive and adhesive failure and when the coating was decreased to 75 µm the 10 mol% geraniol achieved adhesive failure, albeit with large variability. This 1:2 10 mol% geraniol coating showed two modes of adhesive failure, one in which the coating peeled off smoothly and a second with much larger peel forces but a more staccato removal (see Figure S25 for a visual representation). An increase to 20 mol\% geraniol reintroduced cohesive failure, and an increase to 30 mol\% geraniol showed no noticeable improvement. 1:1 exo:-SH ratios were also evaluated with 10-30 mol% geraniol added as a tackifier. The maximum conversion reached was 82% by NMR, a repeatable result under the tested conditions. Following similar trends, when no geraniol was present the failure mode was completely adhesive, admittedly at very low forces of 0.09 N/cm. Adding 10 mol% geraniol increase the adhesive peel force to 0.15 N/cm. At 20 mol% geraniol the failure mode was completely cohesive, albeit at higher peel forces of 1.58 N/cm, and 30 mol% geraniol lost nearly all force, with cohesive failure at 0.09 N/cm. A commercial rosin ester tackifier (Sylvalite RE 80HP) was also tested at 10 mol% in both 1:2 and 1:1 exo:-SH systems (Figure S26). At the 1:2 ratio the rosin ester dissolved into solution but the coating clouded up upon drying, indicating a lack of complete miscibility. In the 1:1 system the rosin ester appeared to have better miscibility and increased the adhesive force to 0.14 N/cm. Notably, the optimal performance of geraniol tackifier was typically 10 mol%, significantly lower than the amount of tackifier typically reported. 16,20,46 For further comparison, a commercial sticky note was tested, showing adhesive failure at 0.35 N/cm and demonstrating the potential utility of terpene coatings having similar peel forces.

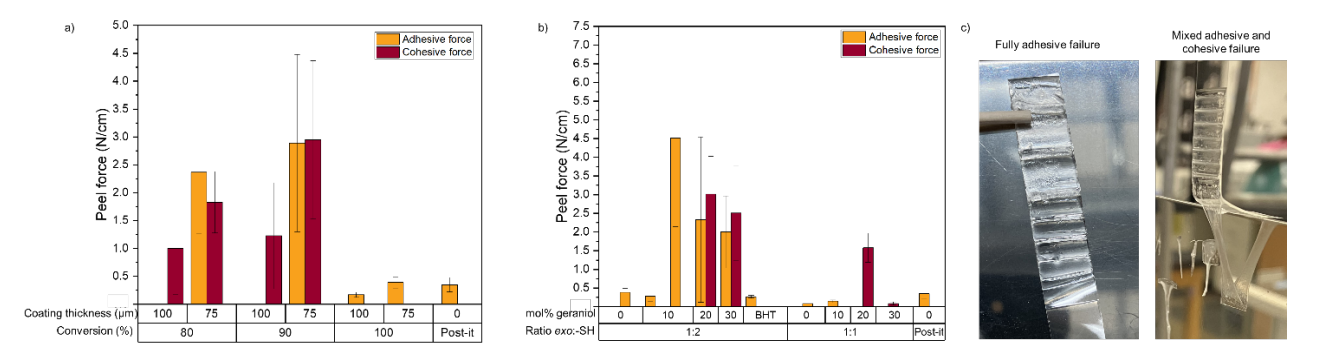


**Figure 2**. a) Peel force values measured for 1:2 *exo*:-SH coatings with varying conversions and coating thicknesses. b) Peel force values for coatings at 75 μm thickness and varying levels of

additive. See Figures S27-29 for representative peel force curves. c) Representative photos of fully adhesive and mixed adhesive/cohesive failure during peel testing

Based on the high  $T_{\rm g}$  values seen for the purified linear polymers, the thermal behavior of the formed coatings was of interest. The TGA curves all showed multi-stage degradations, with systems without geraniol showing an additional degradation stage (Figure S30). Notably, the  $T_{\rm g}$  values are now within the expected range for PSA materials, showing values all at or below 0 °C. Comparing within the 1:2 ratio systems, the addition of geraniol served to depress the  $T_{\rm g}$ , from -8 °C with no geraniol present to -24 °C with 30 mol% geraniol. A similar trend is observed for the 1:1 ratio coatings, showing a decrease from 0.4 °C to -29 °C as the geraniol level increases (Figure S31). While geraniol was added with the intention of tackifying, this depression of the  $T_{\rm g}$  upon its addition suggests a plasticizing effect<sup>11</sup> rather than tackifying occurring.<sup>47</sup> Future work of the rheological behavior of these films could elucidate the precise effects on the modulus, however these effects suggest the addition of geraniol acts more as a plasticizer than a tackifier, while still increasing the adhesion strength.

Recalling that for the purified 1:2 polymers the IR stretch indicated possible disulfide formations, further investigation of potential crosslinking was explored. An IR spectrum of the formed coatings also indicated possible disulfide formations, for both 1:2 and 1:1 coatings, although it is worth noting this stretch is in the fingerprint region and therefore difficult to precisely identify. During NMR investigations, the dried 1:2 coatings showed partial insolubility, again indicating residual crosslinking occurring. A control coating was made with the addition of butylated hydroxytoluene (BHT) after the polymerization to arrest any radical reactions during the drying process. Gel fractions of the 1:2 system with no additive showed a 14% gel fraction remaining for the 1:2 coating, decreasing to 6% when BHT is present (Figure S24). The 1:1 coatings were also tested and showed no gel fraction, consistent with their complete dissolution in solvent. The thermal degradation of the dried 1:2 coating with BHT showed a slightly lower  $T_{d.5\%}$  (121 vs 140 °C) but nearly identical  $T_g$  (-10 vs -8 °C). The peel force dropped slightly from 0.39 N/cm to 0.27 N/cm, mimicking the addition of geraniol. The only difference in the proton NMR spectra was a slight decrease in residual MEK that could be seen for the BHT coating, though the proton NMR spectra are limited to the soluble portion and thus may not be capturing any crosslinking occurring (Figure S23). The IR spectra of dried coatings also only showed a decrease in MEK, suggesting the crosslinking occurring may be difficult to see by IR, such as the formation of disulfide linkages from unreacted thiols (Figure S22). We postulate this light amount of crosslinking is what confers higher peel strengths on the 1:2 coatings in comparison to their 1:1 analogues, given the similar  $M_n$  values seen under experimental conditions.

The degradation of these coatings was studied in 1M HCl, water, and 1M NaOH with acetone or MEK added in as a solvent. The coatings appeared stable in water for several weeks, showing a whitening but no significant mass loss. Coating samples were then placed in 1 M HCl and 1 M NaOH with 50% by volume of acetone, MEK, or no additional solvent doped in, as well as DI water with 50% by volume acetone or MEK doped in. The most significant degradations occurred in acidic systems, with aqueous 1 M HCl degrading all coatings within 4 days (Figure 3, see Figures S33-38 for remaining conditions), a process that was accelerated by the addition of

MEK. The acidic solution appeared to decarboxylate the polycarbonate and hydrolyze any residual alkenes, based on NMR analysis (See Figures S39-40). Overall, these data show an exciting opportunity for these sustainable adhesives to be degraded at the end of their use instead of ending up as plastic waste.

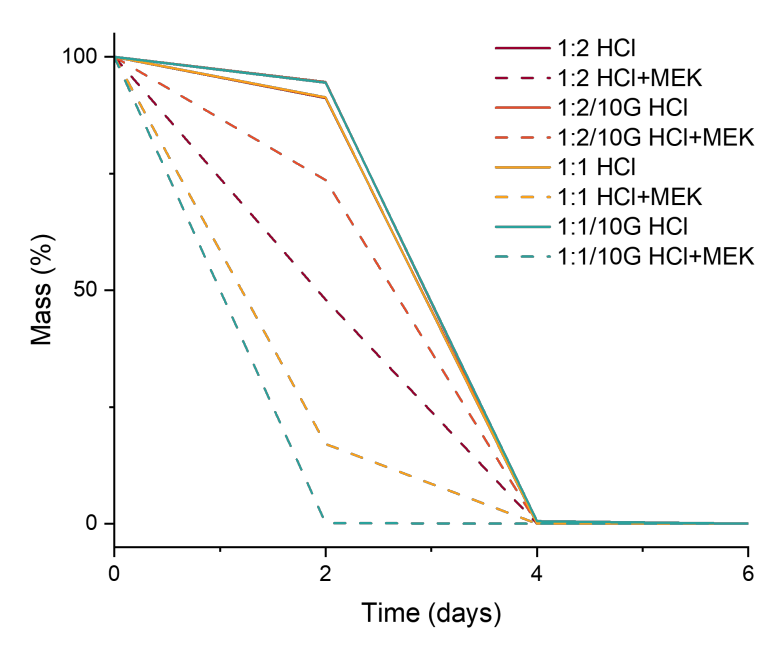


**Figure 3**. Degradation curves for 1:2 and 1:1 coatings in HCl and HCl+MEK

In conclusion, we report on a thiol-ene step-growth polymerization for a carveol-based alkene monomer with renewably-derived DTT and its use as a pressure-sensitive adhesive. Upon polymerization with an excess of thiol the resulting coating shows adhesive failure with peel forces comparable to a commercial sticky note The mode of failure can be tuned from cohesive to adhesive by modulating the coating thickness and the addition of geraniol acting as a plasticizer increases peel forces at as low as 10 mol%. Coatings were degraded in acidic conditions in as little as 2 or 4 days, demonstrating a potential facile end-of-life pathway for carveol-based adhesives. This work introduces an exciting demonstration of using thiol-ene step-growth polymerization for natural product-based terpene-based monomers and their applications as pressure-sensitive adhesives.

# **Acknowledgements:**

This work was funded by the NSF Center for Sustainable Polymers CHE-1901635. We would like to thank Dr. Shuang Liang for their assistance and helpful conversations.

## ASSOCIATED CONTENT

Supporting Information available: Synthesis and characterization, spectra, adhesive curves, and

#### References

- (1) Hayes, G.; Laurel, M.; Mackinnon, D.; Zhao, T.; Houck, H. A.; Becer, C. R. Polymers without Petrochemicals: Sustainable Routes to Conventional Monomers. *Chem Rev* **2022**. https://doi.org/10.1021/acs.chemrev.2c00354.
- (2) Barnes, D. K. A.; Galgani, F.; Thompson, R. C.; Barlaz, M. Accumulation and Fragmentation of Plastic Debris in Global Environments. *Philosophical Transactions of the Royal Society B: Biological Sciences* **2009**, *364* (1526), 1985–1998. https://doi.org/10.1098/rstb.2008.0205.
- (3) Geyer, R.; Jambeck, J. R.; Law, K. L. Production, Use, and Fate of All Plastics Ever Made. *Sci Adv* **2017**, *3*, 25–29. https://doi.org/10.1126/sciadv.1700782.
- (4) Lange, J.; Dusselier, M.; De Wildeman, S. Biodegradable Polymers A Tutorial for a Circular Plastics Economy. *Biodegradable Polymers in the Circular Plastics Economy* **2022**, 1–16. https://doi.org/10.1002/9783527827589.ch1.
- (5) Pradeep, S. V.; Kandasubramanian, B.; Sidharth, S. A Review on Recent Trends in Bio-Based Pressure Sensitive Adhesives. *J Adhes* **2023**, *99* (14), 2145–2166. https://doi.org/10.1080/00218464.2023.2176761.
- (6) Sivasankarapillai, G.; Eslami, E.; Laborie, M. P. Potential of Organosolv Lignin Based Materials in Pressure Sensitive Adhesive Applications. *ACS Sustain Chem Eng* **2019**, *7* (15), 12817–12824. https://doi.org/10.1021/acssuschemeng.9b01670.
- (7) Abu Bakar, R.; Hepburn, K. S.; Keddie, J. L.; Roth, P. J. Degradable, Ultraviolet-Crosslinked Pressure-Sensitive Adhesives Made from Thioester-Functional Acrylate Copolymers. *Angewandte Chemie* **2023**, *135* (34), 1–9. https://doi.org/10.1002/ange.202307009.
- (8) Yamamoto, M.; Nakano, F.; Doi, T.; Moroishi, Y. Synthesis and PSA Performance Study for Novel Acrylic and Butyl Acrylate Block Copolymers. *Int J Adhes Adhes* **2002**, *22* (1), 37–40. https://doi.org/10.1016/S0143-7496(01)00034-3.
- (9) Ding, K.; John, A.; Shin, J.; Lee, Y.; Quinn, T.; Tolman, W. B.; Hillmyer, M. A. High-Performance Pressure-Sensitive Adhesives from Renewable Triblock Copolymers. *Biomacromolecules* **2015**, *16* (8), 2537–2539. https://doi.org/10.1021/acs.biomac.5b00754.
- (10) Gallagher, J. J.; Hillmyer, M. A.; Reineke, T. M. Acrylic Triblock Copolymers Incorporating Isosorbide for Pressure Sensitive Adhesives. *ACS Sustain Chem Eng* **2016**, *4* (6), 3379–3387. https://doi.org/10.1021/acssuschemeng.6b00455.
- (11) Choi, Y. M.; Lee, B. H.; Park, J. W.; Kim, H. J.; Eom, Y. G.; Jang, S. W.; Lee, Y. K. Adhesion Properties of Eco-Friendly PVAc Emulsion Adhesive Using Nonphthalate Plasticizer. *J Adhes Sci Technol* **2013**, 27 (5–6), 536–550. https://doi.org/10.1080/01694243.2012.705481.
- (12) Vendamme, R.; Schüwer, N.; Eevers, W. Recent Synthetic Approaches and Emerging Bio-Inspired Strategies for the Development of Sustainable Pressure-Sensitive Adhesives Derived from

- Renewable Building Blocks. *J Appl Polym Sci* **2014**, *131* (17), 8379–8394. https://doi.org/10.1002/app.40669.
- (13) Droesbeke, M. A.; Aksakal, R.; Simula, A.; Asua, J. M.; Du Prez, F. E. Biobased Acrylic Pressure-Sensitive Adhesives. *Prog Polym Sci* 2021, 117, 101396. https://doi.org/10.1016/j.progpolymsci.2021.101396.
- (14) Albanese, K. R.; Okayama, Y.; Morris, P. T.; Gerst, M.; Gupta, R.; Speros, J. C.; Hawker, C. J.; Choi, C.; De Alaniz, J. R.; Bates, C. M. Building Tunable Degradation into High-Performance Poly(Acrylate) Pressure-Sensitive Adhesives. *ACS Macro Lett* **2023**, *12* (6), 787–793. https://doi.org/10.1021/acsmacrolett.3c00204.
- (15) Ma, Y.; Ji, Y.; Zhang, J.; Sha, Y.; Jia, P.; Zhou, Y. Research Advances in Vegetable-Oil-Based Pressure-Sensitive Adhesives. *Green Mater* **2023**, *11*, 147–161. https://doi.org/10.1680/jgrma.22.00061.
- (16) Sajjad, H.; Tolman, W. B.; Reineke, T. M. Block Copolymer Pressure-Sensitive Adhesives Derived from Fatty Acids and Triacetic Acid Lactone. ACS Appl Polym Mater 2020, 2 (7), 2719–2728. https://doi.org/10.1021/acsapm.0c00317.
- (17) Li, Y.; Sun, X. S. Synthesis and Characterization of Acrylic Polyols and Polymers from Soybean Oils for Pressure-Sensitive Adhesives. *RSC Adv* 2015, 5 (55), 44009–44017. https://doi.org/10.1039/c5ra04399a.
- (18) Lei, Y. F.; Wang, X. L.; Liu, B. W.; Ding, X. M.; Chen, L.; Wang, Y. Z. Fully Bio-Based Pressure-Sensitive Adhesives with High Adhesivity Derived from Epoxidized Soybean Oil and Rosin Acid. *ACS Sustain Chem Eng* **2020**, *8* (35), 13261–13270. https://doi.org/10.1021/acssuschemeng.0c03451.
- (19) Pu, G.; Hauge, D. A.; Gu, C.; Zhang, J.; Severtson, S. J.; Wang, W.; Houtman, C. J. Influence of Acrylated Lactide-Caprolactone Macromonomers on the Performance of High Biomass Content Pressure-Sensitive Adhesives. *Macromol React Eng* **2013**, *7* (10), 515–526. https://doi.org/10.1002/mren.201300160.
- (20) Shin, J.; Martello, M. T.; Shrestha, M.; Wissinger, J. E.; Tolman, W. B.; Hillmyer, M. A. Pressure-Sensitive Adhesives from Renewable Triblock Copolymers. *Macromolecules* **2011**, *44* (1), 87–94. https://doi.org/10.1021/ma102216d.
- (21) Kim, H. J.; Jin, K.; Shim, J.; Dean, W.; Hillmyer, M. A.; Ellison, C. J. Sustainable Triblock Copolymers as Tunable and Degradable Pressure Sensitive Adhesives. *ACS Sustain Chem Eng* **2020**, *8* (32), 12036–12044. https://doi.org/10.1021/acssuschemeng.0c03158.
- (22) Nasiri, M.; Reineke, T. M. Sustainable Glucose-Based Block Copolymers Exhibit Elastomeric and Adhesive Behavior. *Polym Chem* **2016**, *7* (33), 5233–5240. https://doi.org/10.1039/c6py00700g.
- (23) Sajjad, H.; Tolman, W. B.; Reineke, T. M. Block Copolymer Pressure-Sensitive Adhesives Derived from Fatty Acids and Triacetic Acid Lactone. *ACS Appl Polym Mater* **2020**, *2* (7), 2719–2728. https://doi.org/10.1021/acsapm.0c00317.

- (24) Prebihalo, E. A.; Johnson, M.; Reineke, T. M. Bio-Based Thiol-Ene Network Thermosets from Isosorbide and Terpenes. *ACS Macro Lett* **2024**, *13*, 586–591. https://doi.org/10.1021/acsmacrolett.4c00078.
- (25) Nakajima, N.; Babrowicz, R.; Harrell, E. R. Rheology, Composition, and Peel-mechanism of Block Copolymer–Tackifier-based Pressure Sensitive Adhesives. *J Appl Polym Sci* **1992**, *44* (8), 1437–1456. https://doi.org/10.1002/app.1992.070440814.
- (26) Barrueso-Martínez, M. L.; Del Pilar Ferrándiz-Gómez, T.; Romero-Sánchez, M. D.; Martín-Martínez, J. M. Characterization of EVA-Based Adhesives Containing Different Amounts of Rosin Ester or Polyterpene Tackifier. *Journal of Adhesion* **2003**, *79* (8–9), 805–824. https://doi.org/10.1080/00218460309547.
- (27) Mess, A.; Vietzke, J. P.; Rapp, C.; Francke, W. Qualitative Analysis of Tackifier Resins in Pressure Sensitive Adhesives Using Direct Analysis in Real Time Time-of-Flight Mass Spectrometry. *Anal Chem* **2011**, *83* (19), 7323–7330. https://doi.org/10.1021/ac2011608.
- (28) Noppalit, S.; Simula, A.; Billon, L.; Asua, J. M. Paving the Way to Sustainable Waterborne Pressure-Sensitive Adhesives Using Terpene-Based Triblock Copolymers. *ACS Sustain Chem Eng* **2019**, *7* (21), 17990–17998. https://doi.org/10.1021/acssuschemeng.9b04820.
- (29) Noppalit, S.; Simula, A.; Ballard, N.; Callies, X.; Asua, J. M.; Billon, L. Renewable Terpene Derivative as a Biosourced Elastomeric Building Block in the Design of Functional Acrylic Copolymers. *Biomacromolecules* **2019**, *20* (6), 2241–2251. https://doi.org/10.1021/acs.biomac.9b00185.
- (30) Baek, S. S.; Hwang, S. H. Preparation of Biomass-Based Transparent Pressure Sensitive Adhesives for Optically Clear Adhesive and Their Adhesion Performance. *Eur Polym J* **2017**, *92* (April), 97–104. https://doi.org/10.1016/j.eurpolymj.2017.04.039.
- (31) Baek, S.-S.; Jang, S.-H.; Hwang, S.-H. Construction and Adhesion Performance of Biomass Tetrahydro-Geraniol-Based Sustainable/Transparent Pressure Sensitive Adhesives. *Journal of Industrial and Engineering Chemistry* **2017**, *53*, 429–434.
- (32) Droesbeke, M. A.; Simula, A.; Asua, J. M.; Du Prez, F. E. Biosourced Terpenoids for the Development of Sustainable Acrylic Pressure-Sensitive Adhesives: Via Emulsion Polymerisation. *Green Chemistry* **2020**, *22* (14), 4561–4569. https://doi.org/10.1039/d0gc01350a.
- (33) Engelen, S.; Droesbeke, M.; Aksakal, R.; Du Prez, F. E. Ring-Opening Metathesis Polymerization for the Synthesis of Terpenoid-Based Pressure-Sensitive Adhesives. ACS Macro Lett 2022, 11 (12), 1378–1383. https://doi.org/10.1021/acsmacrolett.2c00618.
- (34) Fang, R.; Jiang, C. H.; Wang, X. Y.; Zhang, H. M.; Liu, Z. L.; Zhou, L.; Du, S. S.; Deng, Z. W. Insecticidal Activity of Essential Oil of Carum Carvi Fruits from China and Its Main Components against Two Grain Storage Insects. *Molecules* 2010, 15 (12), 9391–9402. https://doi.org/10.3390/molecules15129391.
- (35) Serafim, C. A. de L.; Araruna, M. E. C.; Alves Júnior, E. B.; Silva, L. M. O.; Silva, A. O.; da Silva, M. S.; Alves, A. F.; Araújo, A. A.; Batista, L. M. (-)-Carveol Prevents Gastric Ulcers via Cytoprotective,

- Antioxidant, Antisecretory and Immunoregulatory Mechanisms in Animal Models. *Front Pharmacol* **2021**, *12* (August), 1–17. https://doi.org/10.3389/fphar.2021.736829.
- (36) Prebihalo, E. A.; Johnson, M.; Reineke, T. M. Bio-Based Thiol-Ene Network Thermosets from Isosorbide and Terpenes. *ACS Macro Lett* **2024**, *13*, 586–591. https://doi.org/10.1021/acsmacrolett.4c00078.
- (37) Sarapas, J. M.; Tew, G. N. Thiol-Ene Step-Growth as a Versatile Route to Functional Polymers. *Angewandte Chemie* **2016**, *128* (51), 16092–16095. https://doi.org/10.1002/ange.201609023.
- (38) Sarapas, J. M.; Tew, G. N. Poly(Ether-Thioethers) by Thiol-Ene Click and Their Oxidized Analogues as Lithium Polymer Electrolytes. *Macromolecules* **2016**, *49* (4), 1154–1162. https://doi.org/10.1021/acs.macromol.5b02513.
- (39) Lillie, L. M.; Tolman, W. B.; Reineke, T. M. Degradable and Renewably-Sourced Poly(Ester-Thioethers) by Photo-Initiated Thiol-Ene Polymerization. *Polym Chem* **2018**, *9* (23), 3272–3278. https://doi.org/10.1039/c8py00502h.
- (40) Masnabadi, N.; Ghasemi, M. H.; Beyki, M. H.; Sadeghinia, M. Oxidative Dimerization of Thiols to Disulfide Using Recyclable Magnetic Nanoparticles. *Research on Chemical Intermediates* **2017**, *43* (3), 1609–1618. https://doi.org/10.1007/s11164-016-2718-1.
- (41) Taniguchi, M.; Iizuka, J.; Murata, Y.; Ito, Y.; Iwamiya, M.; Mori, H.; Hirata, Y.; Mukai, Y.; Mikuni-Takagaki, Y. Multimolecular Salivary Mucin Complex Is Altered in Saliva of Cigarette Smokers: Detection of Disulfide Bridges by Raman Spectroscopy. *Biomed Res Int* **2013**, *2013*, 168765. https://doi.org/10.1155/2013/168765.
- (42) Deubel, F.; Bretzler, V.; Holzner, R.; Helbich, T.; Nuyken, O.; Rieger, B.; Jordan, R. Polythioethers by Thiol-Ene Click Polyaddition of α,ω-Alkylene Thiols. *Macromol Rapid Commun* **2013**, *34* (12), 1020–1025. https://doi.org/10.1002/marc.201300265.
- (43) Lindner, A.; Lestriez, B.; Mariot, S.; Creton, C.; Maevis, T.; Lühmann, B.; Brummer, R. Adhesive and Rheological Properties of Lightly Crosslinked Model Acrylic Networks. *Journal of Adhesion* **2006**, 82 (3), 267–310. https://doi.org/10.1080/00218460600646594.
- (44) Abu Bakar, R.; Hepburn, K. S.; Keddie, J. L.; Roth, P. J. Degradable, Ultraviolet-Crosslinked Pressure-Sensitive Adhesives Made from Thioester-Functional Acrylate Copolymers. *Angewandte Chemie* **2023**, *135* (34), 1–9. https://doi.org/10.1002/ange.202307009.
- (45) Wenzel, F.; Agirre, A.; Aguirre, M.; Leiza, J. R. Incorporation of Novel Degradable Oligoester Crosslinkers into Waterborne Pressure Sensitive Adhesives: Towards Removable Adhesives. *Green Chemistry* **2020**, *22* (10), 3272–3282. https://doi.org/10.1039/d0gc00463d.
- (46) Ewert, T. R.; Mannion, A. M.; Coughlin, M. L.; Macosko, C. W.; Bates, F. S. Influence of Rheology on Renewable Pressure-Sensitive Adhesives from a Triblock Copolymer. *J Rheol (N Y N Y)* 2018, 62 (1), 161–170. https://doi.org/10.1122/1.5009194.
- (47) Kraus, G.; Rollmann, K. W.; Gray, R. A. Tack and Viscoelasticity of Block Copolymer Based Adhesives. *J Adhes* **1979**, *10* (3), 221–236. https://doi.org/10.1080/00218467908544626.